

Shunt estimation in pneumonia of different aetiologies: a non-invasive physiological assessment

Federico Raimondi ,¹ Luca Novelli ,¹ Luca Malandrino,¹ Simone Pappacena,² Giuseppe F Sferrazza Papa,³ Antonio Caronni,^{4,5} Laura Perucca,^{4,5} Gianmariano Marchesi,⁶ Gianluca Milanese,⁷ Maurizio Balbi,⁸ Fabiano Di Marco ^{1,9}

To cite: Raimondi F, Novelli L, Malandrino L, *et al*. Shunt estimation in pneumonia of different aetiologies: a non-invasive physiological assessment. *BMJ Open Respir Res* 2026;**13**:e003929. doi:10.1136/bmjresp-2025-003929

Received 8 November 2025
Accepted 12 February 2026

ABSTRACT

Introduction COVID-19 has challenged traditional models of respiratory failure, and several studies have suggested that gas exchange impairment in COVID-19 pneumonia may involve mechanisms beyond anatomical shunt. This has renewed interest in non-invasive physiological tools to explore gas exchange abnormalities, including the evaluation of shunt, dead space and ventilation/perfusion mismatch.

Material and methods This prospective cross-sectional study was conducted between October 2020 and January 2021 at Papa Giovanni XXIII Hospital (Bergamo, Italy), enrolling adults with acute respiratory failure due to COVID-19 or other pneumonias. Pulmonary shunt fraction was estimated non-invasively via the BEACON system using peripheral oxygen saturation (SpO₂)/fraction of inspired oxygen responses during incremental oxygen steps. Chest CT scans were quantitatively analysed for pathological patterns. The primary outcome was the comparison of BEACON-estimated shunt fraction between COVID-19 and non-COVID-19 groups; the secondary outcome included correlations with CT findings.

Results A total of 51 patients were enrolled, including 36 with COVID-19 and 15 with non-COVID-19 pneumonia. COVID-19 patients showed significantly higher pulmonary shunt fractions (18.2% vs 12.5%, $p=0.022$). In non-COVID-19 cases, shunt fraction correlated positively with the extent of CT consolidations ($p=0.567$, $p=0.035$) and negatively with ground-glass opacities ($p=-0.565$, $p=0.035$). No significant correlations between shunt and CT findings were observed in COVID-19 patients.

Conclusions Our findings demonstrate increased estimated shunt in COVID-19 pneumonia despite comparable radiological severity to non-COVID-19 pneumonias, reinforcing the concept of distinct gas exchange pathophysiology across different pneumonia aetiologies.

INTRODUCTION

COVID-19 has profoundly challenged classical paradigms of acute respiratory failure (ARF). Early in the pandemic, clinicians observed that some patients with COVID-19 pneumonia presented with profound hypoxaemia despite

WHAT IS ALREADY KNOWN ON THIS TOPIC

⇒ Pulmonary gas exchange, particularly shunt, can be assessed non-invasively through the analysis of the oxyhaemoglobin dissociation curve and the behaviour of oxygen saturation in response to fraction of inspired oxygen changes. The multiple inert gas elimination technique remains the physiological gold standard for the assessment of shunt and ventilation/perfusion relationships. These principles can be applied to characterise different pneumonia aetiologies.

WHAT THIS STUDY ADDS

⇒ A mismatch was observed between radiological impairment and estimated shunt values, which—despite comparable imaging findings—were higher in SARS-CoV-2 than in other pneumonia, suggesting an aetiology-specific disturbance in gas exchange mechanisms.

HOW THIS STUDY MIGHT AFFECT RESEARCH, PRACTICE OR POLICY

⇒ Pneumonias are currently classified according to epidemiological, anatomical or severity-based criteria. This study suggests the addition of a pathophysiological dimension focused on gas exchange mechanisms, which could refine diagnostic phenotyping and, in the long term, possibly support more targeted therapeutic approaches.

relatively preserved lung compliance and limited radiological involvement—features that differ substantially from traditional acute respiratory distress syndrome (ARDS).^{1–3} This atypical phenotype, often referred to as COVID-19-associated ARDS (C-ARDS), has prompted renewed interest in the underlying mechanisms of gas exchange impairment, particularly the contribution of ventilation/perfusion (V/Q) mismatch and intrapulmonary shunt.⁴

In this context, the pandemic has revived the clinical application of physiological tools



© Author(s) (or their employer(s)) 2026. Re-use permitted under CC BY-NC. No commercial re-use. See rights and permissions. Published by BMJ Group.

For numbered affiliations see end of article.

Correspondence to
Dr Luca Novelli;
lnovelli@asst-pg23.it



previously confined to research settings or limited clinical application.⁵ Among these, the analysis of the shape and trajectory of the peripheral oxygen saturation (SpO₂) curve in response to incremental fraction of inspired oxygen (FIO₂) adjustments has gained renewed attention as a simple and non-invasive method to evaluate the components of gas exchange impairment—namely, intrapulmonary shunt, dead space and V/Q mismatch.⁶

In classic ARDS, hypoxaemia is primarily attributed to anatomical shunt due to perfusion of non-aerated alveoli, a phenomenon typically proportional to the extent of radiological consolidation.⁷ However, in COVID-19, several lines of evidence have suggested a potential role for microvascular dysregulation, pulmonary microthrombosis and intrapulmonary vascular shunting as additional mechanisms contributing to hypoxaemia.^{8–11} These discrepancies have stimulated the implementation of non-invasive gas exchange evaluation methods, aiming to better characterise the underlying physiological alterations in COVID-19-related respiratory failure.

This study aimed to estimate the pulmonary shunt fraction by a non-invasive method in patients with pneumonia due to COVID-19 and other aetiologies. In addition, it investigated the relationship between shunt magnitude and baseline CT patterns.

MATERIAL AND METHODS

Study design and patient population

This was a prospective cross-sectional study conducted between October 2020 and January 2021 at Papa Giovanni XXIII Hospital (Bergamo, Italy), a large tertiary care centre in Northern Italy. The study was approved by the local Ethics Committee (Comitato Etico di Bergamo, Resolution No. 2215/2020) and written or verbal informed consent was obtained from all participants in accordance with local regulations in place at the time.

Adult patients hospitalised with ARF due to either SARS-CoV-2 infection or other suspected infectious aetiologies were prospectively enrolled. According to the institutional protocol in place during the study period, all consecutive adult patients admitted to the sub-intensive respiratory care unit with a clinical diagnosis of pneumonia who met predefined inclusion and exclusion criteria were included, without postenrolment exclusions. Admission criteria included failure of a continuous positive airway pressure (CPAP) trial—defined as an arterial partial pressure of oxygen (PaO₂)/FIO₂ (PF) ratio <200 mm Hg, worsening gas exchange or a respiratory rate >30 breaths per minute. All included patients were haemodynamically stable and able to cooperate with non-invasive physiological assessments, including arterial line placement, spontaneous breathing trials and incremental FIO₂ adjustments. Consequently, the study population did not include critically ill or deeply sedated patients requiring invasive mechanical ventilation. The non-COVID-19 group was conceived as a pragmatic clinical comparator and included consecutive patients

with ARF due to pneumonia not caused by SARS-CoV-2, all meeting the same inclusion criteria and requiring management in a respiratory high-dependency unit.

Patient involvement

Patients were not involved in defining the research question or study design. However, they were informed about the rationale and purpose of the physiological measurements and how these data could advance clinical research. Due to the pandemic context and patients' critical conditions, extrahospital involvement was not feasible. Family members were informed and involved when requested by the patients.

Clinical and ancillary data collection

Collected data included anthropometric parameters, smoking history and the date of SARS-CoV-2 PCR positivity when applicable. All patients underwent chest CT and arterial line placement for serial arterial blood gas analysis. Patients with chronic lung disease requiring long-term oxygen therapy or home non-invasive ventilation were excluded. Pulmonary thromboembolism, when identified, was recorded but excluded from the final analysis.

Pulmonary shunt measurement

Pulmonary shunt fraction was assessed using a non-invasive, tablet-based platform (BEACON CareSystem, Mermaid Care A/S, Denmark), which builds on the physiological principles, algorithms and technological advancements of the Automated Lung Parameter Estimator system.¹² The BEACON system estimates pulmonary shunt and V/Q mismatch by analysing the shape and trajectory of the SpO₂ curve in response to incremental FIO₂ adjustments.

The BEACON system integrates a gas analyser, a pulse oximeter and proprietary software to characterise pulmonary gas exchange. The assessment involves step-wise adjustments of FIO₂ over 4–6 steps across approximately 15–20 min, aiming to cover a target SpO₂ range of 90–100%, with patients connected via an oronasal face-mask. For each FIO₂ step, steady-state conditions were automatically identified by the BEACON system based on stability of end-tidal oxygen, after which the corresponding SpO₂-FIO₂ data point was recorded and the system prompted progression to the next FIO₂ level.

Shunt impairs oxygenation by allowing deoxygenated blood to bypass ventilated alveoli, resulting in hypoxaemia with limited responsiveness to increases in FIO₂ and a characteristic downward displacement of the SpO₂-FIO₂ relationship, from which intrapulmonary shunt fraction (expressed as a percentage of cardiac output) can be estimated. In contrast, V/Q mismatch is reflected by a rightward shift of the SpO₂-FIO₂ curve and typically improves with higher FIO₂ levels. These mechanisms are quantified by fitting patient-specific SpO₂-FIO₂

data to a physiological model, yielding an estimate of pulmonary shunt. All physiological measurements were performed in spontaneous breathing at zero end-expiratory pressure. During the BEACON assessment, the facemask served exclusively as an interface and was connected to a T-piece supplied by an air-oxygen flowmeter; target FIO₂ levels were achieved using standard air/oxygen mixing tables and continuously verified by an independent FIO₂ monitoring sensor placed in the circuit (Criterion Oxichcek, Respironics). Although patients could be receiving different forms of respiratory support (including CPAP or non-invasive ventilation) as part of routine clinical care, BEACON measurements were systematically performed during clinically scheduled breaks from positive-pressure support. This standardised approach minimised the potential influence of positive end expiratory pressure (PEEP).

Chest CT scan analysis

Chest CT scans were performed using a standard-dose protocol, with or without intravenous contrast enhancement, acquired in the supine position at full inspiration. Imaging extended from the lung bases to the apex and was acquired using one of two 64-slice CT scanners (Brilliance, Philips, Amsterdam, Netherlands; CT Evolution, GE Healthcare, Chicago, Illinois, USA). Images were reconstructed using a sharp kernel optimised for lung parenchyma, with slice thickness ranging from 0.9 mm to 1.5 mm.

Digital Imaging and Communications in Medicine data were transferred to a picture archiving and communication system workstation. Two radiologists independently reviewed the CT images using dedicated software (Thoracic VCAR, GE Healthcare, IL, USA).

Initially developed for emphysema quantification in chronic obstructive pulmonary disease, the software has subsequently been applied in several studies to quantify lung parenchymal involvement in COVID-19 pneumonia.^{13–15} During the COVID-19 pandemic, it was therefore used to enable voxel-based classification of lung parenchyma based on predefined Hounsfield Unit (HU) thresholds implemented in the software. A colour-coded map was generated to visualise different radiological patterns: emphysema (–1024 to –977 HU; blue), normally aerated pulmonary parenchyma (–977 to –703 HU; black), ground-glass opacities (GGO; –703 to –368 HU; light pink), ‘other’ parenchymal densities (–368 to –100 HU; white) and consolidations (–100 to +5 HU; red). These values were expressed as percentages of total lung volume for statistical analysis.

Outcomes

The primary outcome was the comparison of pulmonary BEACON-estimated shunt fraction between patients with COVID-19 and those with non-COVID-19 pneumonia. Secondary outcomes included the characterisation of parenchymal abnormalities on baseline chest

CT—specifically the presence and extent of ground-glass opacities and consolidations—and their correlation with the measured shunt fraction.

Statistical analysis

Continuous variables were summarised as medians and IQRs, while categorical variables were reported as absolute counts. Comparisons between the COVID-19 and non-COVID-19 pneumonia groups were performed using the Wilcoxon rank-sum exact test for continuous variables, given the limited sample size in the non-COVID-19 group (n<30) and the non-normal distribution of several variables. Categorical variables were compared using the χ^2 test when expected cell counts were sufficient (n>5); otherwise, Fisher’s exact test was applied.

To visualise group differences in pulmonary shunt, medians and 95% CIs were estimated using non-parametric bootstrap resampling (10 000 iterations). This method was chosen to provide robust interval estimates without relying on distributional assumptions, particularly given the small sample size in the non-COVID-19 group.

The relationship between the percentage of pulmonary shunt and radiological involvement—specifically the percentage of lung affected by ground-glass opacities (GGOs) and consolidations—was assessed using Spearman’s rank correlation coefficient.

A two-sided p value<0.05 was considered statistically significant. No corrections for multiple testing were applied, as this was an exploratory analysis. As a sensitivity analysis addressing aetiological heterogeneity, the primary comparison was repeated after excluding the patient with exogenous lipoid pneumonia from the non-COVID-19 group. The sample size was based on feasibility considerations and, given the exploratory nature of the study, it was not powered a priori to detect a predefined between-group difference. There were no missing values for outcome variables or radiological parameters. Some missing data in demographic variables were left unfilled and are specified in the Results section where clinically relevant. Analyses were performed using R software (V.4.4.2, R Foundation for Statistical Computing, Vienna, Austria) and Jamovi software (V.2.3.28.0).

RESULTS

A total of 51 patients were included in the study. All variables, for both the overall population and the subgroups, are summarised in [table 1](#). The median age was 67 years, and 43 patients (84.3%) were male. The median body mass index was 27.4 kg/m². Regarding smoking history, 28 patients (54.9%) were never smokers, nine (17.6%) were former smokers and seven (13.7%) were current smokers (with seven missing data). The median length of hospital stay (LOS) was 12 days.

Among all included patients, 36 (70.6%) were diagnosed with COVID-19 pneumonia, while the remaining 15 (29.4%) were diagnosed with non-COVID-19 pneumonia.

Table 1 Demographic, clinical, respiratory and CT imaging characteristics in the overall population, COVID-19 and non-COVID-19 pneumonia patients

	Overall population n=51	Non-COVID-19 n=15	COVID-19 n=36	P value
<i>Demographic and clinical</i>				
Age, years	67 (58–78)	65 (55–75)	68 (60–80)	0.341
Sex, males	43 (84.3%)	13 (86.7%)	30 (83.3%)	0.999
BMI, kg/m ²	27.4 (24.1–30.2)	25.7 (24.0–28.3)	28.3 (24.3–31.6)	0.207
Smoker				<0.001
Never	28 (54.9%)	4 (26.7%)	24 (66.7%)	
Former	9 (17.6%)	4 (26.7%)	5 (13.9%)	
Current	7 (13.7%)	7 (46.6%)	0 (0.0%)	
Missing	7 (13.7%)	0 (0.0%)	7 (19.4%)	
LOS, days	12 (8–19)	12 (8–19)	12 (9–18)	0.791
<i>Respiratory</i>				
pH	7.45 (7.43–7.47)	7.46 (7.45–7.48)	7.44 (7.43–7.46)	0.014
PaO ₂ , mm Hg	61.5 (57.4–68.8)	62.8 (58.1–80.5)	61.1 (57.4–67.9)	0.408
PaCO ₂ , mm Hg	35.3 (32.4–38.4)	33.5 (32.2–35.5)	36.7 (32.8–40.7)	0.010
HCO ₃ ⁻ , mmol/L	24.6 (23.7–26.2)	24.0 (22.6–25.6)	24.9 (24.1–26.4)	0.066
PaO ₂ /FIO ₂	255 (163–297)	269 (201–296)	251 (162–297)	0.476
Shunt, (% of CO)	16.8 (11.8–23.1)	12.5 (5.0–17.5)	18.2 (12.8–24.0)	0.022
<i>CT scan volume</i>				
Normal, cm ³	2911 (2266–3730)	3387 (2591–4633)	2692 (2230–3228)	0.124
Normal (%)	74 (62.5–81.9)	79.5 (70.3–85.5)	72.6 (58.6–78.0)	0.184
Consolidation, cm ³	102 (17–363)	108 (10–426)	102 (21–259)	0.868
Consolidation (%)	2.5 (0–7.9)	2.9 (0.0–10.4)	2.5 (0.0–6.1)	1.000
GGO, cm ³	465 (108–881)	146 (15–617)	467 (193–916)	0.231
GGO, (%)	9.2 (3.3–19.2)	3.5 (0.0–15.0)	12.4 (6.3–21.6)	0.080
Reticular, cm ³	119 (45–449)	111 (33–244)	158 (59–580)	0.419
Reticular (%)	2.9 (1.1–13.4)	2.2 (0.0–5.6)	3.8 (1.1–19.4)	0.298
Total volume, cm ³	3747 (3336–4798)	4448 (3476–5438)	3637 (3194–4649)	0.124

No missing data were present for other variables.

CT volumes are expressed as absolute values (cm³) and relative proportions (% of total lung volume).

Bold values indicate $p < 0.05$ and were considered statistically significant.

Continuous variables are expressed as median (IQR).

BMI, body mass index; CO, cardiac output; FIO₂, fraction of inspired oxygen; GGO, ground-glass opacities; HCO₃⁻, bicarbonate; LOS, length of hospital stay; PaCO₂, arterial partial pressure of carbon dioxide; PaO₂, arterial partial pressure of oxygen.

Specifically, the aetiologies of non-COVID-19 pneumonia included: eight cases of *Legionella pneumophila*, three cases of bacterial lobar pneumonia of unspecified aetiology and three cases of SARS-CoV-2-negative interstitial pneumonia, one of which occurred in an HIV-positive patient. One patient had exogenous lipid pneumonia.

No significant differences were observed between the two groups in terms of demographic and clinical characteristics, except for smoking history, with current smoking being markedly more frequent in the non-COVID-19 group.

In terms of respiratory status on hospital admission, most patients exhibited hypoxaemic normohypocapnic

respiratory failure. Specifically, the median arterial pH was 7.45, PaO₂ was 61.5 mm Hg, arterial partial pressure of carbon dioxide (PaCO₂) was 35.3 mm Hg, and bicarbonate was 24.6 mmol/L. The PF ratio was 255 (163–297).

At the time of admission to the respiratory high-dependency unit, where shunt measurements were performed, patients with COVID-19 pneumonia showed significantly higher BEACON-estimated shunt fractions compared with those with non-COVID-19 pneumonia (median 18.2% (12.8–24.0) vs 12.5% (5.0–17.5); $p=0.022$; see [table 1](#) and [figure 1](#)). In a sensitivity analysis excluding the patient with exogenous lipid pneumonia—whose diagnosis was established retrospectively, after initial

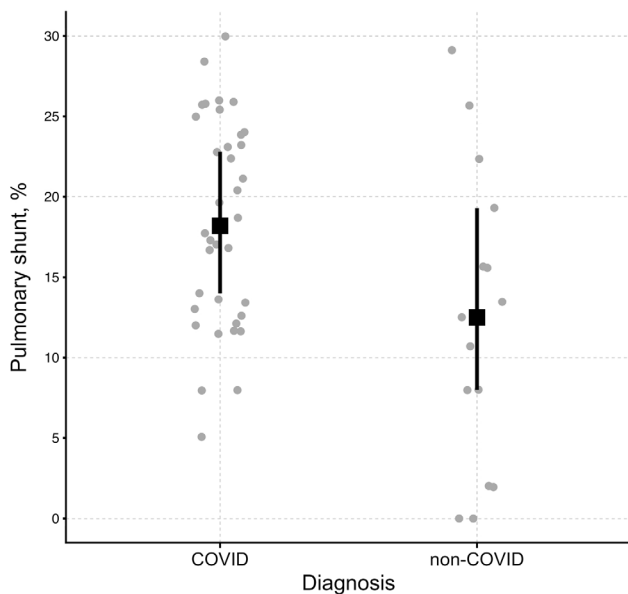


Figure 1 Pulmonary shunt in COVID-19 and non-COVID-19 pneumonia Individual patient values are shown as grey dots. Black squares represent group medians, with vertical bars indicating the 95% CI estimated by non-parametric bootstrap (10 000 resamples). Pulmonary shunt was significantly higher in COVID-19 than in non-COVID-19 pneumonia (Wilcoxon rank-sum exact test, $p=0.022$).

presentation with suspected infectious pneumonia—the difference in pulmonary shunt between COVID-19 and non-COVID-19 pneumonia remained statistically significant (median 18.2% (12.8–24.0) vs 13.0% (3.5–18.4); Mann-Whitney U test, $p=0.041$). Additionally, COVID-19 patients had significantly higher PaCO₂ values (36.7 mm Hg vs 33.5 mm Hg, $p=0.010$) and a less alkalotic pH (7.44 vs 7.46, $p=0.014$).

Chest CT was performed in all patients prior to physiological assessment. The time interval between chest CT acquisition and physiological assessment was ≤ 48 hours in the majority of cases, with 45% of patients undergoing CT within 24 hours. The median extent of abnormal parenchyma was 26% (IQR: 18.1–37.5%). GGOs represented the most prevalent abnormality, with a median volume of 9.2% (IQR: 3.3–19.2%) of the total lung, followed by reticulations (2.9% (IQR: 1.1–13.4%)) and consolidations (2.5% (IQR: 0.7–9.6%)). Total lung volumes, the proportion of normal parenchyma (74% (IQR: 62.5–81.9%)) and the distribution of radiological abnormalities (GGO, consolidations and reticulations) did not significantly differ between COVID-19 and non-COVID-19 groups.

In the overall population, no significant correlations were observed between shunt fraction and either the percentage of lung volume occupied by GGO (Spearman's $\rho=-0.176$, $p=0.258$) or consolidations ($\rho=0.278$, $p=0.071$).

When analysed separately, divergent trends emerged between COVID-19 and non-COVID-19 pneumonia

patients. In non-COVID-19 cases, the shunt fraction showed a significant moderate positive correlation with the extent of consolidation ($\rho=0.567$, $p=0.035$) and a significant moderate negative correlation with GGO volume ($\rho=-0.565$, $p=0.035$). These correlations were not visually pronounced due to data dispersion but remained statistically significant (figure 2). In contrast, no significant associations were found in the COVID-19 group (consolidation: $\rho=0.051$, $p=0.793$; GGO: $\rho=-0.109$, $p=0.572$).

DISCUSSION

In this study, we report a significantly higher pulmonary shunt fraction in patients with COVID-19 pneumonia compared with those with non-COVID-19 pneumonia. Notably, higher shunt values in COVID-19 pneumonia were observed despite a comparable extent and pattern of radiological involvement between groups, suggesting a dissociation between structural lung abnormalities and gas exchange impairment. This finding supports the concept that different pneumonia aetiologies may share similar radiological appearances while exhibiting distinct physiological mechanisms of hypoxaemia. The clinical implications and the specific pathophysiological mechanisms underlying these observations remain to be clarified and were beyond the scope of the present study.

Regarding the other statistically significant differences observed between groups, the association with smoking is difficult to interpret due to seven missing values in the COVID-19 group. COVID-19 patients also showed slightly higher PaCO₂ and a less alkalotic pH; however, these differences were modest, not clinically relevant and consistent with the previous literature.¹⁶ Therefore, our discussion focuses primarily on the observed difference in shunt fraction.

Historically, hypoxaemia in ARDS is attributed to anatomical shunt, that is, perfusion of non-aerated alveoli, which correlates with the extent of radiological consolidation and is unresponsive to increased FIO₂.^{3 17} Classic physiological studies using the multiple inert gas elimination technique have shown that hypoxaemia in pneumonia may result from variable contributions of shunt and V/Q mismatch, depending on disease severity and phenotype.¹⁸ However, early clinical observations in COVID-19 challenged this view. Profound hypoxaemia was noted even in the presence of relatively preserved lung compliance and mild-to-moderate parenchymal involvement.¹ Several hypotheses involving the microvasculature have been proposed. Histopathological analyses of lungs affected by COVID-19 frequently reveal marked pulmonary vascular involvement, including diffuse endothelial injury, widespread microthrombosis and signs of aberrant angiogenesis.^{8 19 20} Moreover, microvascular dysfunction and capillary obstruction can reduce capillary transit time (TT), potentially impairing the equilibration of O₂ across the alveolar-capillary membrane. When the TT becomes critically short, oxygen may not

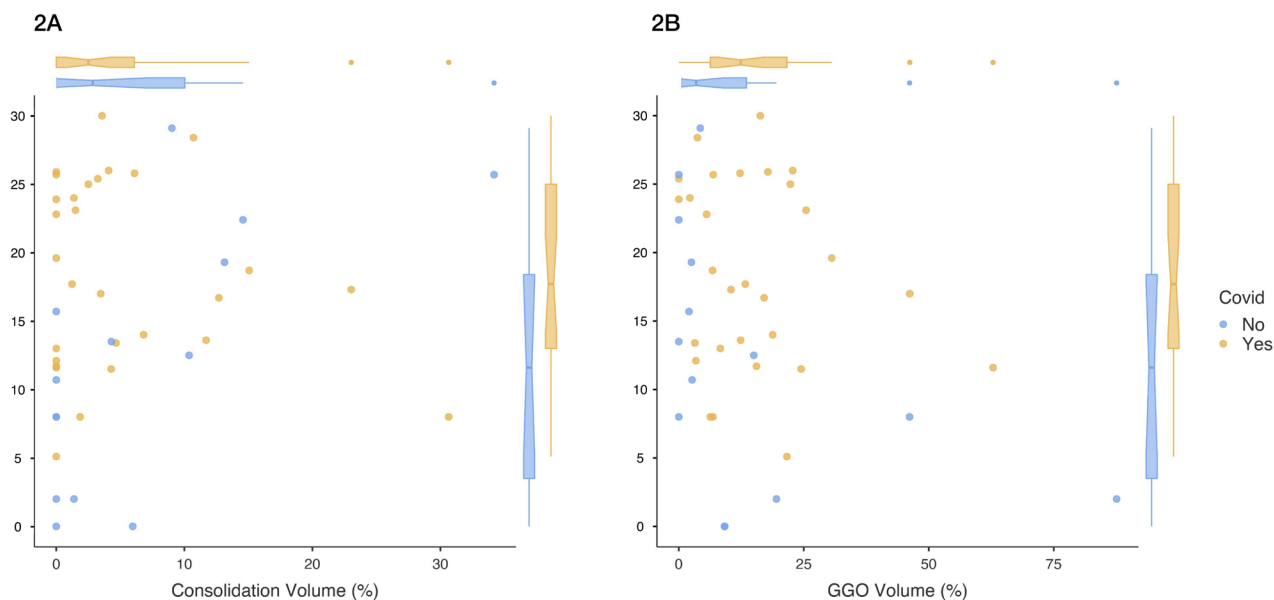


Figure 2 Relationship between pulmonary shunt and radiological lung involvement. Scatterplots show the association between estimated pulmonary shunt fraction and (A) consolidation volume (%) and (B) ground-glass opacity volume (%), stratified by diagnosis (COVID-19 in yellow; non-COVID-19 pneumonia in blue). No regression lines are shown, as correlations were assessed using Spearman's rank coefficient (ρ), which does not assume linearity. Marginal boxplots summarise the distribution of shunt values within each group.

fully equilibrate even in ventilated alveoli, effectively mimicking or amplifying the physiological shunt. Such mechanisms have been proposed as potential contributors to gas exchange impairment in COVID-19 and may be consistent with the elevated shunt fractions observed in our cohort.²¹

Regarding shunt estimation and CT imaging, Santini *et al* demonstrated that in one-third of mechanically ventilated patients with C-ARDS, venous admixture exceeded CT-derived anatomical shunt, suggesting the involvement of additional mechanisms such as low V/Q mismatch or diffusion limitation.⁴ Galambos *et al* described functional intrapulmonary arteriovenous shunts via bronchopulmonary anastomoses, contributing to right-to-left shunt. These microvascular shunts appear to be dilated and hyperperfused and may represent a radiologically silent contributor to hypoxaemia.¹¹

Our findings, both in terms of increased shunt and the lack of correlation with consolidative or ground-glass patterns in COVID-19 pneumonia, are consistent with these observations, possibly reflecting the contribution of additional mechanisms beyond parenchymal involvement. Conversely, in non-COVID-19 pneumonia, the shunt fraction showed a positive correlation with the extent of consolidation and a negative correlation with ground-glass volume. This pattern likely reflects the more classical pathophysiology of bacterial pneumonia, in which predominantly interstitial involvement does not significantly impair gas exchange through shunt mechanisms. However, these correlations in the non-COVID-19

subgroup should be interpreted with caution, given the limited sample size, and are therefore presented as exploratory observations. Given the challenges of investigating such discrepancies in vivo, the COVID-19 pandemic renewed interest in longstanding physiological models designed to characterise respiratory failure in terms of shunt, dead space and V/Q mismatch.^{5 22 23} Several non-invasive techniques of varying complexity have been developed over time for this purpose. These methods typically rely on the analysis of inspired, expired and arterial partial pressures of O₂ and CO₂, combined with peripheral oxygen saturation measurements. Simpler approaches use a single measurement at room air (FIO₂ 21%) to estimate shunt and dead space with reasonable accuracy. More complex methods, including the one employed in our study, involve controlled variations in FIO₂ across multiple steps, enabling a more precise estimation of shunt fraction.

Among the experiences with such techniques, the work by Harbut *et al* is noteworthy: using a single-point evaluation during the acute phase of COVID-19, they reported a median shunt of 10.4% (range 0–22.0%) and alveolar dead space (as a percentage of tidal volume) of 14.9% (range 0–32.3%).²⁴ Scaramuzza *et al* employed the BEACON system to investigate V/Q mismatch at different PEEP levels in intubated COVID-19 patients, observing heterogeneous shunt responses to PEEP adjustments.⁶ These findings highlight the complexity of gas exchange abnormalities in COVID-19 and may help explain the variability in patients' responses to oxygen therapy and ventilatory support.

Kotwica *et al* retrospectively estimated shunt fraction in COVID-19 patients by generating oxygen dissociation curves from bedside pulse oximetry data, using SpO₂ and FIO₂ values recorded at triage and 6 hours later. They reported a median shunt of 14% (4–21%), which is comparable to the values observed in our study median 18.2% (12.8–24.0%). Furthermore, they found a negative prognostic value of shunt in terms of mortality.²⁵ We expanded on this line of research by including a non-COVID-19 control group and by performing real-time measurements of SpO₂, PaO₂ and FIO₂, improving the accuracy of shunt estimation compared with retrospective approaches.

Nonetheless, not all studies agree on the presence of increased shunt levels in COVID-19 pneumonia, and the topic remains controversial. Lau *et al* found no evidence of increased right-to-left shunt rates in COVID-19 patients compared with non-COVID-19 controls (17.0% vs 22.7%, respectively; risk difference –5.7%; 95% CI –18.4 to 7.0; p=0.38). However, in that study, patients were critically ill ICU patients at an advanced stage of respiratory failure, already intubated and compared with other intubated and mechanically ventilated ARDS patients.²⁶ It is possible that at such an advanced stage of disease, whether COVID-19 or not, these differences become less apparent.

In this research framework, our study contributes by prospectively comparing COVID-19 and non-COVID-19 pneumonia using a shared non-invasive method, reinforced by the inclusion of a control group and the parallel assessment of radiological involvement. Although the non-COVID-19 cohort included different infectious aetiologies, sensitivity analyses excluding non-infectious cases confirmed the robustness of the main findings. This approach remains clinically relevant beyond the pandemic context, as it underscores the need for a deeper understanding of the mechanisms underlying respiratory failure, as recently emphasised by Hughes in a European Respiratory Journal editorial.²⁷ Several limitations should be acknowledged. The sample size was relatively small, comparable to other exploratory physiological investigations, and the study was conducted at a single centre. Chest CT scans were not always performed contemporaneously with the physiological assessment, with a variable time interval between imaging and shunt estimation. However, more than half of the CT examinations were performed within 48 hours of the physiological evaluation, and the large majority of these were performed within 24 hours. Given the dynamic evolution of radiological findings, temporal mismatch may still have influenced the strength of associations between CT-derived parameters and physiological measurements, which were therefore considered a secondary objective of the study. In addition, CT analysis was based on voxel classification using fixed HU thresholds, which represent density compartments rather than strict radiological entities. This approach may be affected by overlap between parenchymal patterns and by non-parenchymal

components, potentially leading to misclassification. Smoking status differed significantly between COVID-19 and non-COVID-19 patients and may represent a potential confounder. Given the small sample size, the presence of missing values and the marked imbalance in current smoking prevalence between groups, multivariable adjustment was not feasible and between-group comparisons should be interpreted with caution. Although the BEACON system allows estimation of both intrapulmonary shunt and V/Q mismatch, only shunt was analysed in this study. The lack of V/Q mismatch assessment represents a limitation, as this parameter may provide complementary insights into gas exchange abnormalities. Lastly, the BEACON system is not universally validated, particularly for non-invasive applications.

In conclusion, our findings demonstrate increased estimated shunt in COVID-19 pneumonia despite comparable radiological severity to non-COVID-19 pneumonias, reinforcing the concept of distinct gas exchange pathophysiology across different pneumonia aetiologies. These results highlight the need for further investigation into the mechanisms of respiratory failure using available non-invasive tools. This approach may support phenotypic characterisation, improve hypoxaemia stratification and refine indications for oxygen and ventilatory support, particularly in patients with discordant radiological and clinical findings.

Author affiliations

¹Respiratory Unit, Medicine Department, ASST Papa Giovanni XXIII, Bergamo, Italy

²Don Gnocchi Foundation, Milan, Lombardy, Italy

³Department of Neurorehabilitation Sciences, Casa di Cura Igea, Milan, Lombardy, Italy

⁴Department of Neurorehabilitation Sciences, IRCCS Istituto Auxologico Italiano, Milan, Italy

⁵Department of Biomedical Sciences for Health, University of Milan, Milan, Italy

⁶General Intensive Care Unit, ASST Papa Giovanni XXIII, Bergamo, Italy

⁷Scienze Radiologiche Unit, Department of Medicine and Surgery, University Hospital of Parma, Parma, Italy

⁸Radiology Unit, Department of Oncology, University of Turin, San Luigi Gonzaga Hospital, Orbassano, Italy

⁹Department of Health Sciences, University of Milan, Milan, Italy

Contributors FR, LN, FDM, and GMa conceived and designed the study. FR, LM, SP and GMa performed data collection. FR and AC performed the analysis. MB and GMi analyzed the radiological images. GMi contributed to the manuscript revision process. All authors contributed to data interpretation, critically revised the manuscript for important intellectual content, and approved the final version for submission. Guarantor: FR.

Funding The authors have not declared a specific grant for this research from any funding agency in the public, commercial or not-for-profit sectors.

Competing interests None declared.

Patient and public involvement Patients and/or the public were not involved in the design, conduct, reporting or dissemination plans of this research.

Patient consent for publication Not applicable.

Ethics approval This study involves human participants and was approved by Comitato Etico di Bergamo, Resolution No. 2215/2020. Participants gave informed consent to participate in the study before taking part.

Provenance and peer review Not commissioned; externally peer reviewed.

Data availability statement Data are available upon reasonable request.

Open access This is an open access article distributed in accordance with the Creative Commons Attribution Non Commercial (CC BY-NC 4.0) license, which permits others to distribute, remix, adapt, build upon this work non-commercially, and license their derivative works on different terms, provided the original work is properly cited, appropriate credit is given, any changes made indicated, and the use is non-commercial. See: <https://creativecommons.org/licenses/by-nc/4.0/>.

ORCID iDs

Federico Raimondi <https://orcid.org/0000-0001-9599-6864>

Luca Novelli <https://orcid.org/0000-0002-2705-248X>

Fabiano Di Marco <https://orcid.org/0000-0002-1743-0504>

REFERENCES

- Gattinoni L, Coppola S, Cressoni M, *et al*. COVID-19 Does Not Lead to a "Typical" Acute Respiratory Distress Syndrome. *Am J Respir Crit Care Med* 2020;201:1299–300.
- Bos LDJ, Paulus F, Vlaar APJ, *et al*. Subphenotyping Acute Respiratory Distress Syndrome in Patients with COVID-19: Consequences for Ventilator Management. *Ann Am Thorac Soc* 2020;17:1161–3.
- Pesenti A, Riboni A, Marcolin R, *et al*. Venous admixture (Q_{va}/Q) and true shunt (Q_s/Q_t) in ARF patients: effects of PEEP at constant FIO₂. *Intensive Care Med* 1983;9:307–11.
- Santini A, Protti A, Ferrari M, *et al*. Pathophysiology of hypoxemia in mechanically-ventilated patients with COVID-19: A computed tomography study. *Respir Physiol Neurobiol* 2023;318:104162.
- Wagner PD, Malhotra A, Prisk GK. Using pulmonary gas exchange to estimate shunt and deadspace in lung disease: theoretical approach and practical basis. *J Appl Physiol* 2022;132:1104–13.
- Scaramuzzo G, Karbing DS, Fogagnolo A, *et al*. Heterogeneity of Ventilation/Perfusion Mismatch at Different Levels of PEEP and in Respiratory Mechanics Phenotypes of COVID-19 ARDS. *Respir Care* 2023;68:188–98.
- Bitker L, Talmor D, Richard JC. Imaging the acute respiratory distress syndrome: past, present and future. *Intensive Care Med* 2022;48:995–1008.
- Ackermann M, Verleden SE, Kuehnel M, *et al*. Pulmonary Vascular Endothelialitis, Thrombosis, and Angiogenesis in Covid-19. *N Engl J Med* 2020;383:120–8.
- Bush D, Abman SH, Galambos C. Microvascular Shunts in COVID-19 Pneumonia. *Am J Respir Crit Care Med* 2022;206:227–8.
- Poor HD. Pulmonary Thrombosis and Thromboembolism in COVID-19. *Chest* 2021;160:1471–80.
- Galambos C, Bush D, Abman SH. Intrapulmonary bronchopulmonary anastomoses in COVID-19 respiratory failure. *Eur Respir J* 2021;58:2004397.
- Rees SE, Kjaergaard S, Perthorgaard P, *et al*. The automatic lung parameter estimator (ALPE) system: non-invasive estimation of pulmonary gas exchange parameters in 10-15 minutes. *J Clin Monit Comput* 2002;17:43–52.
- Granata V, Ianniello S, Fusco R, *et al*. Quantitative Analysis of Residual COVID-19 Lung CT Features: Consistency among Two Commercial Software. *J Pers Med* 2021;11:1103.
- Rorat M, Jurek T, Simon K, *et al*. Value of quantitative analysis in lung computed tomography in patients severely ill with COVID-19. *PLoS One* 2021;16:e0251946.
- Belfiore MP, Urraro F, Grassi R, *et al*. Artificial intelligence to codify lung CT in Covid-19 patients. *Radiol Med* 2020;125:500–4.
- Di Mitri C, Arcoleo G, Mazzuca E, *et al*. COVID-19 and non-COVID-19 pneumonia: a comparison. *Ann Med* 2021;53:2321–31.
- Gattinoni L, Caironi P, Cressoni M, *et al*. Lung recruitment in patients with the acute respiratory distress syndrome. *N Engl J Med* 2006;354:1775–86.
- Gea J, Roca J, Torres A, *et al*. Mechanisms of abnormal gas exchange in patients with pneumonia. *Anesthesiology* 1991;75:782–9.
- Leisman DE, Deutschman CS, Legrand M. Facing COVID-19 in the ICU: vascular dysfunction, thrombosis, and dysregulated inflammation. *Intensive Care Med* 2020;46:1105–8.
- Magro C, Mulvey JJ, Berlin D, *et al*. Complement associated microvascular injury and thrombosis in the pathogenesis of severe COVID-19 infection: A report of five cases. *Transl Res* 2020;220:1–13.
- Østergaard L. SARS CoV-2 related microvascular damage and symptoms during and after COVID-19: Consequences of capillary transit-time changes, tissue hypoxia and inflammation. *Physiol Rep* 2021;9:e14726.
- Sapsford DJ, Jones JG. The PIO₂ vs. SpO₂ diagram: a non-invasive measure of pulmonary oxygen exchange. *Eur J Anaesthesiol* 1995;12:375–86.
- Roe PG, Jones JG. Analysis of factors which affect the relationship between inspired oxygen partial pressure and arterial oxygen saturation. *Br J Anaesth* 1993;71:488–94.
- Harbut P, Prisk GK, Lindwall R, *et al*. Intrapulmonary shunt and alveolar dead space in a cohort of patients with acute COVID-19 pneumonitis and early recovery. *Eur Respir J* 2023;61:2201117.
- Kotwica A, Knights H, Mayor N, *et al*. Intrapulmonary shunt measured by bedside pulse oximetry predicts worse outcomes in severe COVID-19. *Eur Respir J* 2021;57:2003841.
- Lau VI, Mah GD, Wang X, *et al*. Intrapulmonary and Intracardiac Shunts in Adult COVID-19 Versus Non-COVID Acute Respiratory Distress Syndrome ICU Patients Using Echocardiography and Contrast Bubble Studies (COVID-Shunt Study): A Prospective, Observational Cohort Study. *Crit Care Med* 2023;51:1023–32.
- Hughes M. Novel gas exchange analysis in COVID-19 lung disease. *Eur Respir J* 2023;61:2201962.